Journal of Electronic Imaging

SPIEDigitalLibrary.org/jei

Local sharpness distribution–based feature points matching algorithm

Yue Zhao
Jianbo Su

Downloaded From: http://electronicimaging.spiedigitallibrary.org/ on 12/18/2014 Terms of Use: http://spiedl.org/terms

Journal of Electronic Imaging 23(1), 013011 (Jan–Feb 2014)

Local sharpness distribution–based feature points matching algorithm

Yue Zhao* **and Jianbo Su**
Shanghai Jiao Tong University and Key Laboratory of System Control and Information Processing, Ministry of Education, Department of Automation, Shanghai 200240, China

Abstract. An efficient descriptor and a complete scheme for removing incorrect correspondences are two essentials for accurate feature points matching in image processing and pattern recognition. This paper proposes a new rigid feature points matching algorithm. First, a new feature descriptor based on the local sharpness distribution is proposed to extract features, which leads to a feature set of extremely low dimensionality. With these features, the normalized cross-correlation coefficient and a bidirectional matching strategy are employed to generate the initial feature point correspondences. Then a complete scheme with two rules is proposed to remove the probable incorrect correspondences. Owing to these two rules based on the voting strategy and the ratio of the distances, respectively, the accuracy of feature points matching is remarkably improved. Experimental results show that the proposed algorithm is efficient for feature matching and comparisons with other algorithms show its better comprehensive performance. *© 2014 SPIE and IS&T* [DOI: 10.1117/1.JEI.23.1.013011]

Keywords: feature points matching; local sharpness distribution; feature point correspondence; normalized cross-correlation coefficient; projective transformation model.

Paper 13438 received Aug. 6, 2013; revised manuscript received Nov. 18, 2013; accepted for publication Dec. 18, 2013; published online Jan. 29, 2014.

1 Introduction

Feature points matching is a fundamental yet still open problem in computer vision research. It is the essential foundation of object recognition, image registration, object tracking, image retrieval, three-dimensional reconstruction, and so on.[1–5]

Various methods for feature points matching have been proposed since the computer vision era began. Yi et al. propose a Harris detector[6–8] based feature points matching algorithm, which employs a normalized cross-correlation coefficient (NCC) matching scheme. Although most of the feature points are correctly matched in Yi's algorithm, some incorrect correspondences are also generated.[9] SUSAN corner detector, proposed by Smith and Brady,[10] is also used to match feature points with high corner localization accuracy and better robustness of enduring the noise. This method employs a circular mask to detect corners and edges but is time consuming in obtaining a SUSAN area and finding corners in large windows.[11] Voss and Suesse[12] present a new feature points matching algorithm, which is a general solution for affine point pattern matching. Chui and Rangarajan[13] investigate nonrigid point matching and propose a scheme to jointly estimate the correspondence and nonrigid transformations between two point-sets of different sizes. Spectral graph analysis technology is used to investigate the correspondence matching of point-sets by Carcassoni and Hancock.[14] Caetano et al. present a novel solution to the rigid point pattern matching problem in Euclidean spaces of any dimension. Their experimental results show improvements in accuracy, particularly when matching patterns of different sizes.[15] Yan et al.[1] propose a feature matching method based on modified projective nonnegative matrix factorization. They project two feature point-sets onto a common subspace using modified projective nonnegative matrix factorization, and then match them in this common subspace. Zhu et al.[16] employ a robust and fast Hausdorff distance method to match images. Compared with the conventional Hausdorff distance method, their method has less computational cost and good robustness for object matching.

To improve the matching accuracy, Qian et al.[17] propose a coarse-to-fine method for feature points (corners) matching. They use multiscale Harris corner detector to extract feature points and then adopt voting-strategy-based matching algorithm to produce the initial pairs of corresponding feature points, followed by a 2-D rigid transformation model constructed for matching the remaining feature points. Good results have been achieved, but there are still some incorrect correspondences. Awrangjeb et al. propose an improved curvature scale-space corner detector,[18–20] which is based on the affine-length parameterization. With this detector, they employ iterative procedures to generate a few of the best matches, which lead to expensive time cost. Consequently, Awrangjeb's algorithm achieves very high matching accuracy. However, its running time is very long.[19,21]

Scale-invariant feature transform (SIFT) descriptor is one of the most well-known feature descriptors.[22] By generating the scale-space, it uses a difference-of-Gaussian function to identify potential interest points which are invariant to scale and orientation. After localizing the keypoints, the orientations are assigned to them. Then, it affords each keypoint a feature descriptor. Finally, it matches feature points using a Euclidean distance metric where a match is rejected if the ratio of the distances that the closest to the second-closest match is greater than a threshold. As the dimensionality of

*Address all correspondence to: Yue Zhao, E-mail: zhaoyue0609@sjtu.edu.cn

0091-3286/2014/$25.00 © 2014 SPIE and IS&T

Downloaded From: http://electronicimaging.spiedigitallibrary.org/ on 12/18/2014 Terms of Use: http://spiedl.org/terms

SIFT feature vector is very large, the time cost for feature points matching is expensive.[5] Besides, SIFT method generates a large number of correspondence pairs with some of them incorrectly matched. Thus, a more complete scheme is further needed to remove the incorrect correspondences by SIFT method.[23]

In order to improve the efficiency of feature points matching and remove the incorrect correspondences, this paper proposes a new rigid feature points matching algorithm. First, a new feature descriptor based on the local sharpness distribution is introduced, which have quite low dimensionality. With these features, the NCC is computed to measure the similarity of feature points from the same scene in two images. Then, a bidirectional matching scheme is employed to generate the initial correspondences. Two rules, based on the voting strategy and the ratio of the distances, respectively, are proposed to remove the probable incorrect correspondences. A projective transformation model is then constructed to search the final corresponding feature points.

The rest of this paper is organized as follows. Section 2 proposes a new descriptor for the feature points. The feature points matching algorithm is presented in Sec. 3. Experiments are reported in Sec. 4 to evaluate the performance of the proposed algorithm, followed by conclusions in Sec. 5.

2 New Feature Descriptor

A new feature descriptor is first proposed based on the local sharpness distribution, as shown in, Refs. 7 and 24.

An edge detector (like Canny, Sobel, and so on) is used to obtain the edge map. Suppose there are z points in the q'th edge S_q:

$$S_q = \{P_1, \ldots, P_i, \ldots, P_z\}, \tag{1}$$

A point $P_i(x_i, y_i)$ is randomly selected as the center. It is moved t points forward and backward, respectively, to get two points $P_{i-t}(x_{i-t}, y_{i-t})$ and $P_{i+t}(x_{i+t}, y_{i+t})$. Figure 1 illustrates the definition and computation method of sharpness.[7,24] In Fig. 1, the outer solid line denotes an edge segment of S_q. The dashed line denotes an arc, which is obtained by circle fitting using three points P_{i-t}, P_i, and P_{i+t}. Point O represents the center of the circle. Integer t is selected from the range of [3, 5] according to the experience.[7,24] As t is very small, the triangle $P_{i-t}P_iP_{i+t}$ can be taken as an isosceles triangle approximately, namely $|P_iP_{i-t}| = |P_iP_{i+t}|$. Thus, the following formula can be derived

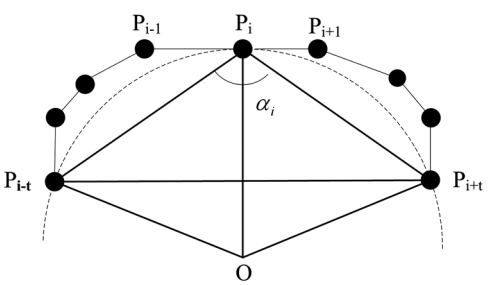

Fig. 1 A visual interpretation for the definition of sharpness.

$$\sin\left(\frac{\alpha_i}{2}\right) = \frac{|P_{i-t}P_{i+t}|/2}{|P_iP_{i-t}|} = \frac{|P_{i-t}P_{i+t}|/2}{|P_iP_{i+t}|} = \frac{|P_{i-t}P_{i+t}|}{|P_iP_{i-t}| + |P_iP_{i+t}|}. \tag{2}$$

By abbreviating the degree of sharpness to sharpness, a sharpness variable can be defined as

$$\text{sharp}_i^q = 1 - \sin\left(\frac{\alpha_i}{2}\right) = 1 - \frac{|P_{i-t}P_{i+t}|}{|P_iP_{i-t}| + |P_iP_{i+t}|}. \tag{3}$$

The variable sharp_i^q denotes the sharpness value of the i'th point in the q'th edge. The range of sharp_i^q is $[0, 1]$, which indicates how sharp the support angle is.

Suppose P_g, the g'th point in the q'th edge, is a center point. It is moved forward and backward sequently to select $2l$ points. Equation (3) is employed to compute the sharpness of the $(2l + 1)$ points, including P_g. Then the local sharpness distribution of P_g is

$$\text{LSD}_g^q = (\text{sharp}_{g-l}, \ldots, \text{sharp}_g, \ldots, \text{sharp}_{g+l}). \tag{4}$$

Its mean value is

$$M_g^q = \sum_{d=-l}^{l} \text{sharp}_{g+d}/(2l+1), \tag{5}$$

and the variance is

$$D_g^q = \sum_{d=-l}^{l} (\text{sharp}_{g+d} - M_g^q)^2/(2l+1). \tag{6}$$

Then, the feature descriptor of P_g can be constructed as

$$L_g^q = (x_g, y_g, M_g^q, D_g^q, g, q), \tag{7}$$

where x_g and y_g are the image coordinates of feature point P_g.

The feature dimensionality is a decisive factor for improving the efficiency of feature point matching.[5] From Eq. (7), we know that the dimensionality of the feature descriptor is only 1×6, which is very low. This greatly contributes to the improvement of the computation efficiency.

3 Feature Points Matching Algorithm

Suppose image $\mathbf{I}$ contains the original feature points, and image $\bar{\mathbf{I}}$ contains the feature points needed to be matched. The corners detected with the method in Ref. 7 are taken as the feature points. The feature descriptor presented in Sec. 2 is employed to extract features for the corners and then a new feature point matching algorithm is proposed to match them.

3.1 *Initial Corner Correspondences*

For image $\mathbf{I}$, the sharpness values of each point in every edge can be computed with Eq. (3). The sharpness values of each point in the m'th edge S_m can be denoted as

$$\text{sharp}^m = (\text{sharp}_1^m, \ldots, \text{sharp}_i^m, \ldots, \text{sharp}_\lambda^m), \tag{8}$$

where λ is the number of the points in the edge S_m.

Downloaded From: http://electronicimaging.spiedigitallibrary.org/ on 12/18/2014 Terms of Use: http://spiedl.org/terms

According to Ref. 7, the points whose sharpness values are larger than an adaptive threshold in one edge are detected as corners. Suppose the corners in the m'th edge can be described as

$$C^m = \{C_1^m, \ldots, C_j^m, \ldots, C_\beta^m\}, \tag{9}$$

where C_j^m denotes the j'th corner in the m'th edge, and β is the total number of the corners in the m'th edge.

Suppose the corresponding point of corner C_j^m in the edge S_m is the i'th point P_i (see Fig. 2). The local sharpness distribution of corner C_j^m (namely, point P_i) is

$$\mathrm{LSD}_i^m = (\mathrm{sharp}_{i-l}^m, \ldots, \mathrm{sharp}_i^m, \ldots, \mathrm{sharp}_{i+l}^m). \tag{10}$$

Then its mean value can be formulated as

$$M_i^m = \sum_{d=-l}^{l} \mathrm{sharp}_{i+d}^m/(2l+1), \tag{11}$$

and the variance is

$$D_i^m = \sum_{d=-l}^{l} (\mathrm{sharp}_{i+d}^m - M_i^m)^2/(2l+1). \tag{12}$$

With Eqs. (11) and (12), the feature descriptor of corner C_j^m is constructed as

$$L_i^m = (x_i, y_i, M_i^m, D_i^m, i, m), \tag{13}$$

where x_i and y_i are the image coordinates of corner C_j^m.

For image $\bar{\mathbf{I}}$, suppose there are w points in the n'th edge $\bar{S}_n$. The sharpness values of the these points are

$$\mathrm{sh\bar{a}rp}^n = (\mathrm{sh\bar{a}rp}_1^n, \ldots, \mathrm{sh\bar{a}rp}_k^n, \ldots, \mathrm{sh\bar{a}rp}_w^n), \tag{14}$$

where $\mathrm{sh\bar{a}rp}_k^n$ is the sharpness value of the k'th point $\bar{P}_k$ in the edge $\bar{S}_n$.

Suppose the corners detected in edge $\bar{S}_n$ are

$$\bar{C}^n = \{\bar{C}_1^n, \ldots, \bar{C}_r^n, \ldots, \bar{C}_h^n\}, \tag{15}$$

where $\bar{C}_r^n$ denotes the r'th corner in the n'th edge, and h is the total number of the corners in the n'th edge of image $\bar{\mathbf{I}}$.

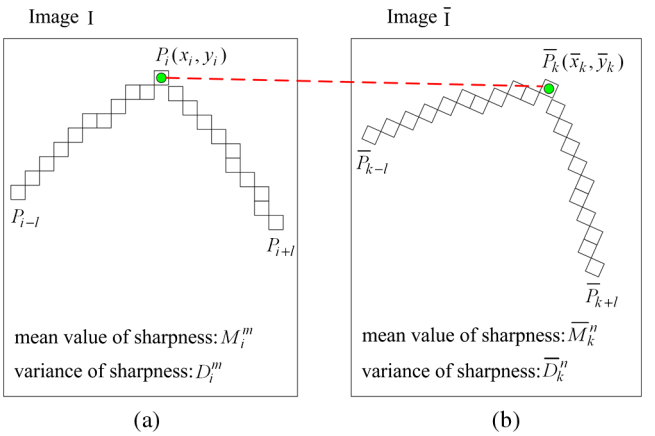

Fig. 2 Examples for the local sharpness distribution of the feature points (marked with a circle): (a) a feature point in the original image and (b) a feature point in the image need to be matched.

If the corresponding point of corner $\bar{C}_r^n$ in the edge $\bar{S}_n$ is the k'th point $\bar{P}_k$ (see Fig. 2), the local sharpness distribution of $\bar{C}_r^n$ is

$$\mathrm{L\bar{S}D}_k^n = (\mathrm{sh\bar{a}rp}_{k-l}^n, \ldots, \mathrm{sh\bar{a}rp}_k^n, \ldots, \mathrm{sh\bar{a}rp}_{k+l}^n). \tag{16}$$

The feature descriptor of corner $\bar{C}_r^n$ can be constructed as

$$\bar{L}_k^n = (\bar{x}_k, \bar{y}_k, \bar{M}_k^n, \bar{D}_k^n, k, n), \tag{17}$$

where $\bar{x}_k$ and $\bar{y}_k$ are the image coordinates of corner $\bar{C}_r^n$.

In order to measure the similarity of two corners in different images, the NCC (Ref. 25) of two different corners, C_j^m and $\bar{C}_r^n$, is computed as

$$R_{jr} = \frac{\sum_{d=-l}^{l}(\mathrm{sharp}_{i+d}^m - M_i^m)(\mathrm{sh\bar{a}rp}_{k+d}^n - \bar{M}_k^n)}{(2l+1)\sqrt{D_i^m \times \bar{D}_k^n}}. \tag{18}$$

A corner from image $\mathbf{I}$ is first selected randomly and then the NCC between this corner and each corner in image $\bar{\mathbf{I}}$ is computed to form one row of NCC matrix R. Repeat this procedure until all the corners in image $\mathbf{I}$ have been selected to compute the NCC for one time. Then, NCC matrix R between the corners in images $\mathbf{I}$ and $\bar{\mathbf{I}}$ is obtained. On the contrary, NCC matrix $\bar{R}$ between the corners in images $\bar{\mathbf{I}}$ and $\mathbf{I}$ is also computed. If R_{jr} and $\bar{R}_{rj}$ are, respectively, the maximums among the j'th row of matrix R and the r'th row of matrix $\bar{R}$, corners C_j^m and $\bar{C}_r^n$ are one initial correspondence pair. With this method, we produce all the initial correspondence pairs between images $\mathbf{I}$ and $\bar{\mathbf{I}}$.

3.2 *Remove the Probable Incorrect Corner Correspondences*

In Sec. 3.1, all the initial correspondence pairs are obtained, which are composed of the original corners in image $\mathbf{I}$ and their corresponding corners in image $\bar{\mathbf{I}}$. Suppose matrix C contains the information of the original corners in image $\mathbf{I}$, and matrix $\bar{C}$ contains the information of the corresponding corners in image $\bar{\mathbf{I}}$. The initial corner correspondences, generated by NCC and a bidirectional matching scheme, contain many incorrect correspondences.[9,17] Thus, we propose two rules for removing the probable incorrect corner correspondences.

Rule 1: If there is only one correspondence pair between the corners of the two edges in image $\mathbf{I}$ and $\bar{\mathbf{I}}$, this correspondence is regraded as a probable incorrect correspondence and will be removed.

For image $\mathbf{I}$, if a corner in the u'th edge of image $\mathbf{I}$ has matched its corresponding corner in image $\bar{\mathbf{I}}$, we cast a vote for the u'th edge. This process is also applied for the remaining corners of C, i.e., the voting score of one edge is equal to the number of the corners in this edge being successfully matched. Finally, a voting matrix T of v edges in image $\mathbf{I}$ is obtained

$$T = (t_1, \ldots, t_u, \ldots, t_v), \tag{19}$$

where t_u is the voting score of the u'th edge. If the u'th edge gains only one score, the corner in the u'th edge is probably matched incorrectly, and it will be deleted from the matrix C. Also, its corresponding corner from matrix $\bar{C}$ is deleted, i.e., a probable incorrect correspondence is removed.

Downloaded From: http://electronicimaging.spiedigitallibrary.org/ on 12/18/2014 Terms of Use: http://spiedl.org/terms

After removing the probable incorrect correspondences from matrixes C and $\bar{C}$, two new matrixes C' and $\bar{C}'$ are obtained

$$\mathbf{C}' = \begin{bmatrix} x_1 & y_1 & p_1 & e_1 & r_1 \\ \vdots & \vdots & \vdots & \vdots & \vdots \\ x_f & y_f & p_f & e_f & r_f \\ \vdots & \vdots & \vdots & \vdots & \vdots \\ x_l & y_l & p_l & e_l & r_l \end{bmatrix}, \tag{20}$$

$$\bar{\mathbf{C}}' = \begin{bmatrix} \bar{x}_1 & \bar{y}_1 & \bar{p}_1 & \bar{e}_1 & \bar{r}_1 \\ \vdots & \vdots & \vdots & \vdots & \vdots \\ \bar{x}_f & \bar{y}_f & \bar{p}_f & \bar{e}_f & \bar{r}_f \\ \vdots & \vdots & \vdots & \vdots & \vdots \\ \bar{x}_l & \bar{y}_l & \bar{p}_l & \bar{e}_l & \bar{r}_l \end{bmatrix}, \tag{21}$$

where x_f and y_f are the image coordinates of the f'th corner in C'; e_f is the ordinal number of the edge that the f'th corner belongs to; p_f is the ordinal number of the corresponding point of f'th corner in the edge e_f; r_f denotes the NCC between the f'th corner in matrix C' and the f'th corner in matrix $\bar{C}'$. $\bar{x}_f$, $\bar{y}_f$, $\bar{p}_f$, $\bar{e}_f$ and $\bar{r}_f$ have the similar meaning with x_f, y_f, p_f, e_f and r_f, respectively. They afford the feature information about the f'th corner in image $\bar{\mathbf{I}}$.

Rule 2: Take two correspondence pairs with the top two largest sums of NCCs as the reference corners. From the remaining correspondence pairs, select one correspondence pair as the one that needs to determine whether the two corners of it are matched correctly. These correspondence pair corners are regarded as candidate corners. For images $\mathbf{I}$ and $\bar{\mathbf{I}}$, the distances between the candidate corner and the two reference corners are, respectively, computed, followed by the ratio of two distances being calculated. If the absolute value of the difference between 1 and the quotient of the two ratios (from images $\mathbf{I}$ and $\bar{\mathbf{I}}$, respectively) is smaller than a threshold set manually, this correspondence is probably incorrect and will be removed.

Adding the fifth columns in matrix C' and $\bar{C}'$, we get the sums

$$\mathbf{r} = \begin{bmatrix} r_1 + \bar{r}_1 \\ \vdots \\ r_f + \bar{r}_f \\ \vdots \\ r_l + \bar{r}_l \end{bmatrix}. \tag{22}$$

For example, suppose the elements r_m and r_n are the top two largest elements in $\mathbf{r}$. Corners A and B, the m'th and n'th corners in C', corners $\bar{A}$ and $\bar{B}$, the m'th and n'th corners in $\bar{C}'$, are taken as the reference corners (Fig. 3). The i'th corner is selected from the remaining corners in matrix C' randomly (namely, corner D). Correspondingly, corner $\bar{D}$, the i'th corner in matrix $\bar{C}'$, is also selected to compute the distance in image $\bar{\mathbf{I}}$.

The ratio of the two distances between corner D to the two reference corners A and B can be computed as

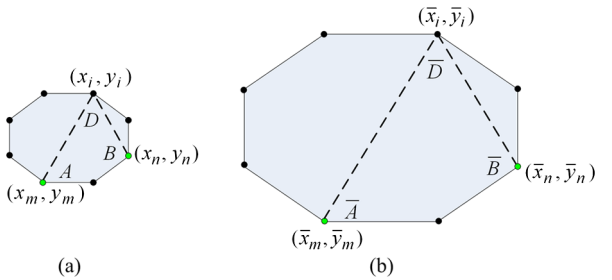

Fig. 3 A visualization of rule 2; A, B, $\bar{A}$, and $\bar{B}$ are reference corners; D is an original corner; and $\bar{D}$ is a corner needed to be matched. (a) the original image and (b) the image needed to be matched.

$$rd_1 = \frac{\sqrt{(x_m - x_i)^2 + (y_m - y_i)^2}}{\sqrt{(x_n - x_i)^2 + (y_n - y_i)^2}}. \tag{23}$$

In image $\bar{\mathbf{I}}$, the ratio of the two distances between the corner $\bar{D}$ to the two reference corners $\bar{A}$ and $\bar{B}$ can be calculated as

$$rd_2 = \frac{\sqrt{(\bar{x}_m - \bar{x}_i)^2 + (\bar{y}_m - \bar{y}_i)^2}}{\sqrt{(\bar{x}_n - \bar{x}_i)^2 + (\bar{y}_n - \bar{y}_i)^2}}. \tag{24}$$

The ratio of rd_1 to rd_2 is

$$rd = \frac{rd_1}{rd_2} = \frac{\sqrt{(x_m - x_i)^2 + (y_m - y_i)^2} \cdot \sqrt{(\bar{x}_n - \bar{x}_i)^2 + (\bar{y}_n - \bar{y}_i)^2}}{\sqrt{(x_n - x_i)^2 + (y_n - y_i)^2} \cdot \sqrt{(\bar{x}_m - \bar{x}_i)^2 + (\bar{y}_m - \bar{y}_i)^2}}. \tag{25}$$

A threshold for $|rd - 1|$ is set manually to determine whether the initial corner correspondence is incorrect. The range of the threshold is [0.01, 0.1]. The smaller the threshold is, the smaller the number of the final correspondence pairs obtained. However, if the threshold becomes too large, the feature point matching accuracy will decrease. If $|rd - 1|$ is larger than the threshold, the initial corner correspondence is probably incorrect and could be removed. By removing the probable incorrect correspondences following these two rules, the remaining correspondence pairs are the most probably correctly matched.

3.3 *Projective Transformation Model*

With the corner correspondences obtained in Sec. 3.2, we construct the projective transformation model which is employed to transform the coordinates of the corners of image $\mathbf{I}$ into that of image $\bar{\mathbf{I}}$.

According to the projective transformation model, the relationship between the coordinates of the original point and the projected point can be expressed by the following equation:

$$s \begin{bmatrix} x_i \\ y_i \\ 1 \end{bmatrix} = \begin{bmatrix} h_1 & h_2 & h_3 \\ h_4 & h_5 & h_6 \\ h_7 & h_8 & h_9 \end{bmatrix} \cdot \begin{bmatrix} \bar{x}_i \\ \bar{y}_i \\ 1 \end{bmatrix} = \mathbf{H} \cdot \begin{bmatrix} \bar{x}_i \\ \bar{y}_i \\ 1 \end{bmatrix}, \tag{26}$$

where (x_i, y_i) is the coordinates of the original point, and $(\bar{x}_i, \bar{y}_i)$ is the coordinates of the projected point.

Downloaded From: http://electronicimaging.spiedigitallibrary.org/ on 12/18/2014 Terms of Use: http://spiedl.org/terms

With at least four correspondence pairs obtained in Sec. 3.2, Eq. (26) can be solved. Then, the parameters matrix H is obtained.

3.4 *Search the Corresponding Corner*

Suppose all the corners detected in image $\mathbf{I}$ and $\bar{\mathbf{I}}$, respectively, are

$$\mathbf{CO} = \begin{bmatrix} x_1 & y_1 \\ \vdots & \vdots \\ x_\rho & y_\rho \\ \vdots & \vdots \\ x_\sigma & y_\sigma \end{bmatrix}, \tag{27}$$

$$\hat{\mathbf{CO}} = \begin{bmatrix} \bar{x}_1 & \bar{y}_1 \\ \vdots & \vdots \\ \bar{x}_s & \bar{y}_s \\ \vdots & \vdots \\ \bar{x}_b & \bar{y}_b \end{bmatrix}, \tag{28}$$

where CO and $\hat{\mathrm{CO}}$ are the corner matrixes of image $\mathbf{I}$ and $\bar{\mathbf{I}}$, respectively. x_ρ and y_ρ are the coordinates of the ρ'th corner in image $\mathbf{I}$. σ is the total number of the corners in image $\mathbf{I}$. $\bar{x}_s$ and $\bar{y}_s$ are the coordinates of the s'th corner in image $\bar{\mathbf{I}}$. b is the total number of the corners in image $\bar{\mathbf{I}}$.

Choose a corner from the matrix CO, and suppose it is the i'th corner (x_i, y_i) of image $\mathbf{I}$. The coordinates of the corresponding corner of corner (x_i, y_i) in image $\bar{\mathbf{I}}$ can be obtained by the projective transformation model Eq. (26) as

$$\begin{cases} \hat{x}_i = \dfrac{(h_2 - h_8 x_i)(y_i - h_6) - (h_5 - h_8 y_i)(x_i - h_3)}{(h_2 - h_8 x_i)(h_4 - h_7 y_i) - (h_5 - h_8 y_i)(h_1 - h_7 x_i)} \\ \hat{y}_i = \dfrac{(h_1 - h_7 x_i)(y_i - h_6) - (h_4 - h_7 y_i)(x_i - h_3)}{(h_1 - h_7 x_i)(h_5 - h_8 y_i) - (h_4 - h_7 y_i)(h_2 - h_8 x_i)} \end{cases}. \tag{29}$$

With the coordinates $(\hat{x}_i, \hat{y}_i)$, we search the closest point to $(\hat{x}_i, \hat{y}_i)$ in matrix $\hat{\mathrm{CO}}$. If one corner has the closest distance to point $(\hat{x}_i, \hat{y}_i)$, and the distance is smaller than a threshold set manually, this corner is taken as the final corresponding corner of (x_i, y_i). With the same steps, we can search the corresponding corners in image $\bar{\mathbf{I}}$ for all the corners in the image $\mathbf{I}$, which produces the final correspondences and finishes the feature point matching between two images.

4 Experiments

To evaluate the performance of the proposed algorithm, the quantitative comparison experiments between the proposed algorithm, Qian's algorithm[17] and Awrangjeb's algorithm[18,19] are implemented first. Then, the qualitative

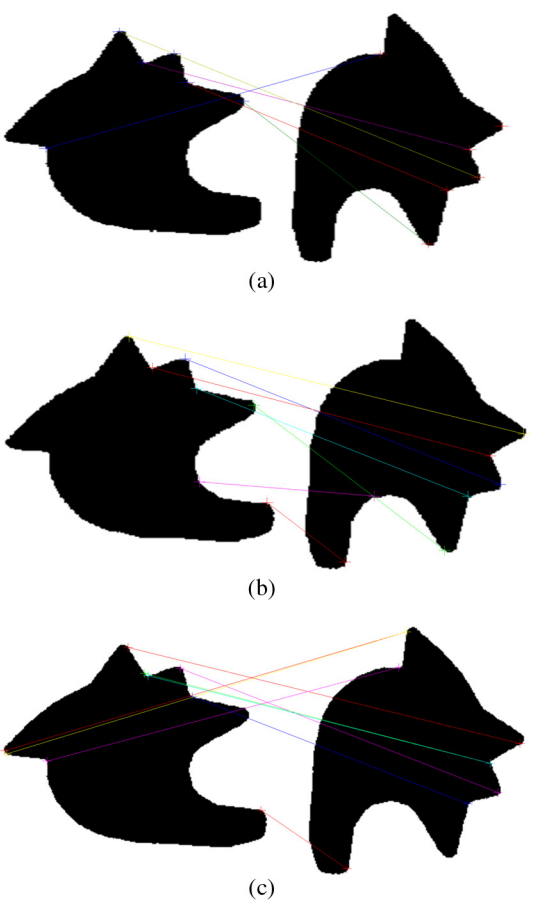

Fig. 4 Compare the corner matching results of Qian's algorithm, Awrangjeb's algorithm and the proposed algorithm on the first pair of binary images: (a) result of Qian's algorithm; (b) result of Awrangjeb's algorithm; and (c) result of the proposed algorithm.

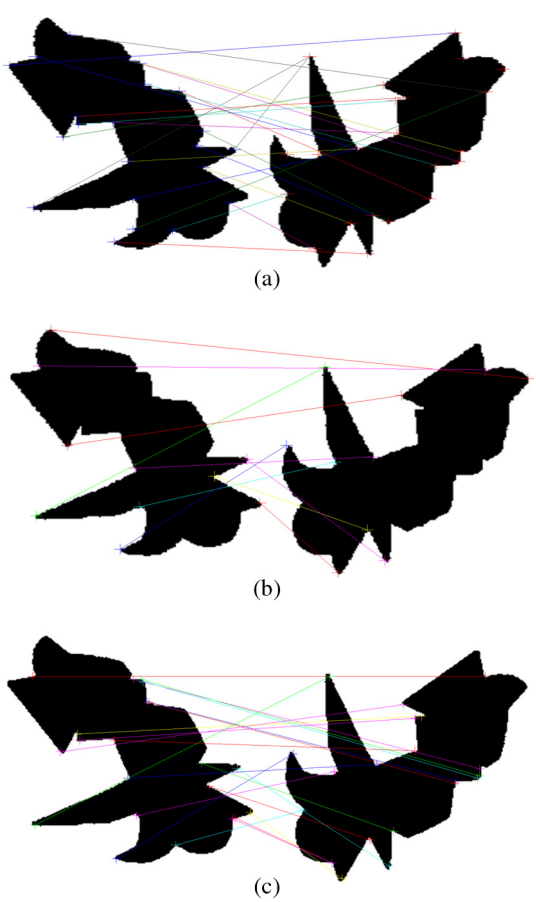

Fig. 5 Compare the corner matching results of Qian's algorithm, Awrangjeb's algorithm and the proposed algorithm on the second pair of binary images: (a) result of Qian's algorithm; (b) result of Awrangjeb's algorithm; and (c) result of the proposed algorithm.

Downloaded From: http://electronicimaging.spiedigitallibrary.org/ on 12/18/2014 Terms of Use: http://spiedl.org/terms

comparison experiments between the proposed algorithm and SIFT algorithm[22] are performed. All the algorithms are implemented in MATLAB R14 on a Four-Core (2.67GHZ) PC.

4.1 *Quantitative Comparison*

To make a quantitative comparison on the proposed algorithm, Qian's algorithm and Awrangjeb's algorithm,[18,19] four pairs of binary images with rotations are adopted to perform the experiments. In our experiments, the reference solutions of the corner correspondences are manually generated, which are identified in an appropriately magnified version of the images. In this way, we can judge whether the correspondence pairs are matched correctly. We also test the running time of the three algorithms. For each pair of binary images, the program is performed for 10 times and then the average running time is calculated. The experimental results are summarized in Figs. 4–7 and Tables 1 and 2.

Figure 4 shows that the Qian's algorithm produces five correct correspondence pairs, whereas the proposed algorithm and Awrangjeb's algorithm both generate seven correct correspondence pairs. Figure 5 indicates that the proposed algorithm generates the largest number of correct correspondence pairs, which is 20. In Fig. 6, the numbers of the correct correspondence pairs of the three algorithms are close to each other, but Qian's algorithm incorrectly generates four correspondence pairs, which is the largest one. From Fig. 7, the proposed algorithm has the largest number of the correct correspondence pairs. Although Awrangjeb's algorithm correctly matches all correspondence pairs, the number of the correct correspondence pairs is only 16.

Comparing the total performance of the three algorithms in Table 1, we can see that the proposed algorithm correctly matches 64 correspondence pairs. Awrangjeb's algorithm has the highest matching accuracy, but the number of the correct correspondence pairs is the smallest. Qian's algorithm has the lowest matching accuracy.

Table 2 presents the running time of the three algorithms. Qian's algorithm costs the shortest running time, and the proposed algorithm is very similar to it in this aspect. Awrangjeb's algorithm consumes much more time than other two algorithms.

By respectively considering the performance in three aspects: the number of correct correspondence pairs, matching accuracy and running time, we can make a comprehensive evaluation for the three algorithms. Qian's

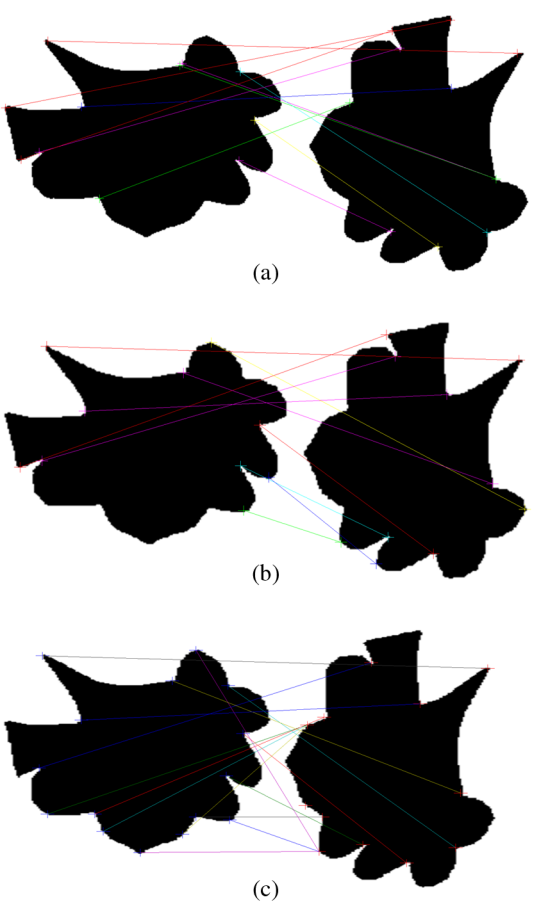

Fig. 6 Compare the corner matching results of Qian's algorithm, Awrangjeb's algorithm and the proposed algorithm on the third pair of binary images: (a) result of Qian's algorithm; (b) result of Awrangjeb's algorithm; and (c) result of the proposed algorithm.

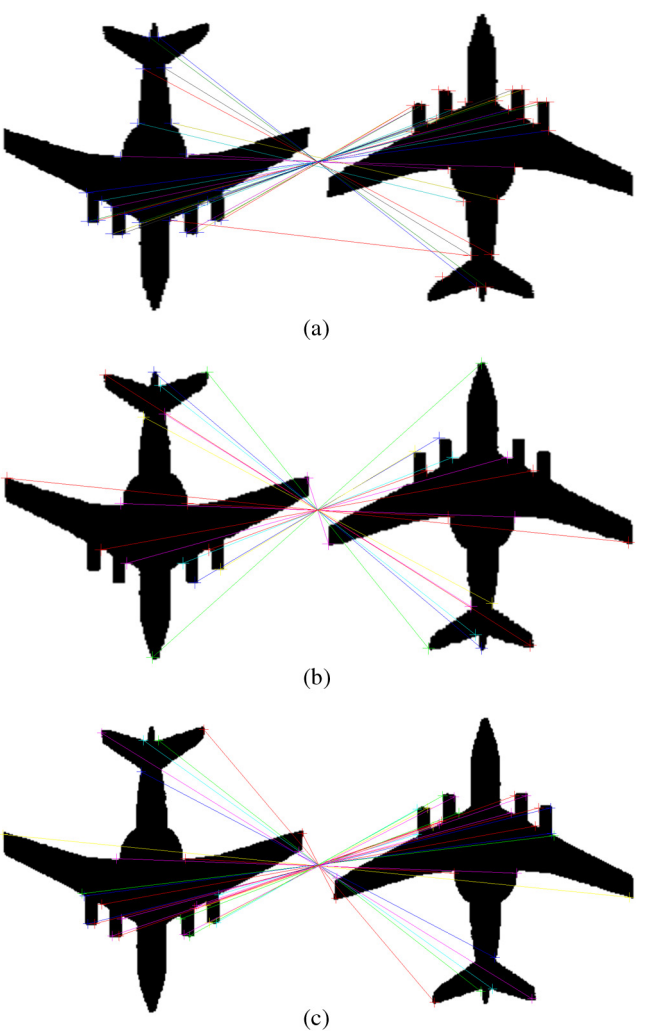

Fig. 7 Compare the corner matching results of Qian's algorithm, Awrangjeb's algorithm and the proposed algorithm on the fourth pair of binary images: (a) result of Qian's algorithm; (b) result of Awrangjeb's algorithm; and (c) result of the proposed algorithm.

Downloaded From: http://electronicimaging.spiedigitallibrary.org/ on 12/18/2014 Terms of Use: http://spiedl.org/terms

Table 1 Matching results evaluation on binary images.

Algorithm	Correspondence Pairs	Correct Correspondence pairs	Matching Accuracy
First pair of binary images			
Qian's (Ref. 17)	6	5	83.33%
Awrangjeb's (Refs. 18 and 19)	7	7	100%
Proposed	9	7	77.78%
Second pair of binary images			
Qian's (Ref. 17)	22	17	77.27%
Awrangjeb's (Ref. 18 and 19)	10	10	100%
Proposed	21	20	95.24%
Third pair of binary images			
Qian's (Ref. 17)	15	11	73.33%
Awrangjeb's (Refs. 18 and 19)	10	10	100%
Proposed	11	10	90.90%
Fourth pair of binary images			
Qian's (Ref. 17)	26	23	88.46%
Awrangjeb's (Refs. 18 and 19)	16	16	100%
Proposed	27	27	100%
Total performance			
Qian's (Ref. 17)	69	56	81.6%
Awrangjeb's (Refs. 18 and 19)	43	43	100%
Proposed	68	64	94.12%

algorithm has the shortest running time, but its matching accuracy is the lowest one. For Awrangjeb's algorithm, it has the highest matching accuracy, but its time cost is the most expensive. Particularly, the running time is 222.45 s in the fourth pair of binary images. It is too long to put up with it. The reason for the results of Awrangjeb's algorithm is that this algorithm employs iterative procedures to generate a few of best matches for high matching accuracy, but these iterative procedures simultaneously greatly increase the time cost. The proposed algorithm generates the largest number of correct correspondence pairs, and its matching accuracy is very close to the best one, so does its running time.

Table 2 Running time comparison on binary images.

Algorithm	Running time (s)
First pair of binary images	
Qian's (Ref. 17)	0.61
Awrangjeb's (Refs. 18 and 19)	1.43
Proposed	1.01
Second pair of binary images	
Qian's (Ref. 17)	0.62
Awrangjeb's (Refs. 18 and 19)	4.05
Proposed	1.10
Third pair of binary images	
Qian's (Ref. 17)	0.66
Awrangjeb's (Refs. 18 and 19)	8.57
Proposed	1.05
Fourth pair of binary images	
Qian's (Ref. 17)	0.66
Awrangjeb's (Refs. 18 and 9)	222.45
Proposed	1.20

Thus, the proposed algorithm has the best comprehensive performance among the three algorithms.

4.2 *Qualitative Comparison*

In this subsection, two pairs of color images taken from different views in the same scene are selected to evaluate the performance of the proposed algorithm. For qualitative comparison, SIFT algorithm[22] is also implemented in these experiments. Experimental results are summarized in Figs. 8 and 9. It should be noted that for rigid point matching between two face images, they should contain variations as few as possible in expression.

From Figs. 8 and 9, we can see that SIFT algorithm generates too many correspondence pairs. Besides that, a lot of correspondence pairs are incorrectly matched. The most obviously incorrect correspondence pairs are shown in the elliptical areas of Figs. 8(a) and 9(a). Meanwhile, the number of the correspondence pairs of the proposed algorithm is not so large as that of the SIFT algorithm, and the proposed algorithm has very high matching accuracy. More importantly, the proposed algorithm extracts feature points from the corner areas while SIFT algorithm has no preference to the corners. The feature points extracted from the corner areas will have great importance, because the corners can afford abundant information for such as real-time gesture recognition, face detection and recognition, robot navigation and image content retrieval.[26,27]

Downloaded From: http://electronicimaging.spiedigitallibrary.org/ on 12/18/2014 Terms of Use: http://spiedl.org/terms

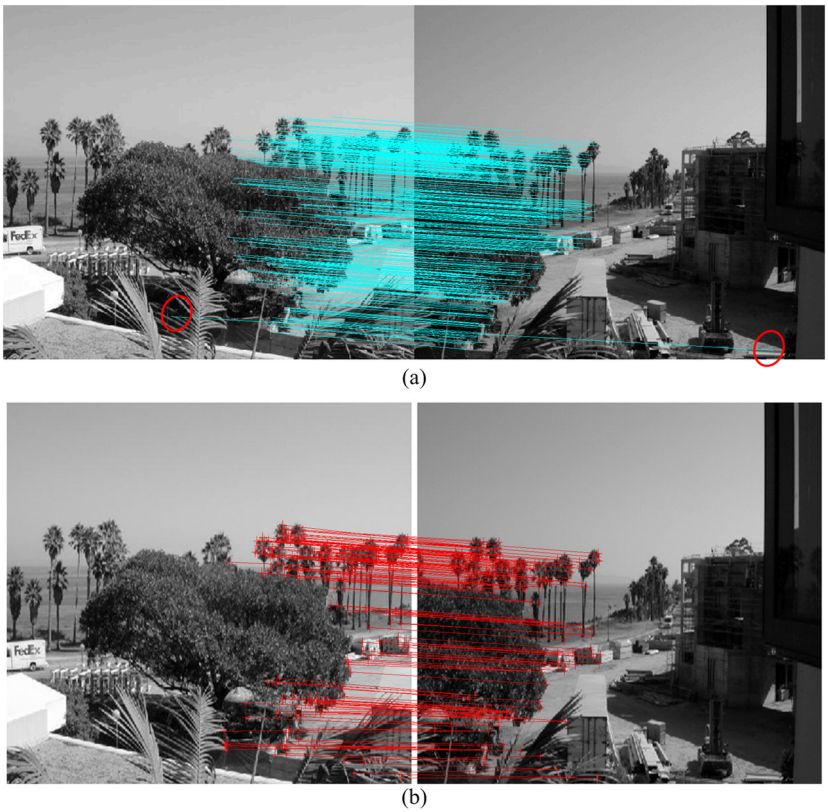

Fig. 8 Compare the corner matching results of scale-invariant feature transform (SIFT) algorithm and the proposed algorithm on the first pair of color images: (a) result of SIFT algorithm and (b) result of the proposed algorithm.

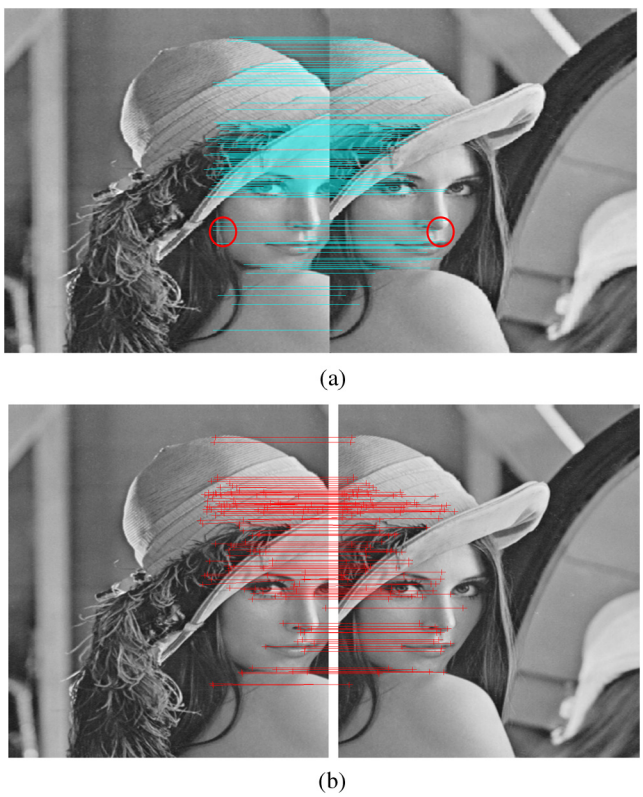

Fig. 9 Compare the corner matching results of SIFT algorithm and the proposed algorithm on the second pair of color images: (a) result of SIFT algorithm and (b) result of the proposed algorithm.

5 Conclusions

This paper focuses on the rigid feature points matching, for which a new matching algorithm is proposed. It first presents a new feature descriptor based on the local sharpness distribution of the feature point to extract features. The dimensionality of the features is extremely low, which greatly improves the efficiency of the feature points matching.

After generating the initial feature point correspondences, two rules are proposed to remove the probable incorrect correspondences: one is based on the voting strategy and the other is based on the ratio of the distances. By removing the probable incorrect feature point correspondences, a projective transformation model with high precision is constructed. The feature points can be accurately matched with this model.

The quantitative and qualitative comparison of experimental results show that the proposed algorithm outperforms other compared algorithms on the comprehensive performance of feature points matching. We really believe that the proposed algorithm can be successfully applied in the image processing area of object recognition, image registration, object tracking, image retrieval, three-dimensional reconstruction, and so on. In the future work, we will make our efforts to improve the scale invariance of our algorithm.

Acknowledgments

This work was partially supported by NSF of China under the grants 60935001 and 61221003.

Downloaded From: http://electronicimaging.spiedigitallibrary.org/ on 12/18/2014 Terms of Use: http://spiedl.org/terms

References

1. W. Yan et al., "Feature matching using modified projective nonnegative matrix factorization," *J. Electron. Imaging* **21**(1), 013005 (2012).
2. J. Ma et al., "Robust estimation of nonrigid transformation for point set registration," in *Proc. IEEE Conf. Computer Vision and Pattern Recognition*, IEEE, Portland, Oregon (2013).
3. Y. Ge et al., "Image registration based on subpixel localization and cauchy–schwarz divergence," *J. Electron. Imaging* **19**(3), 033014 (2010).
4. S. Adhyapak, N. Kehtarnavaz, and M. Nadin, "Stereo matching via selective multiple windows," *J. Electron. Imaging* **16**(1), 013012 (2007).
5. C. Strecha et al., "Ldahash: improved matching with smaller descriptors," *IEEE Trans. Pattern Anal. Mach. Intell.* **34**(1), 66–78 (2012).
6. C. Harris and M. Stephens, "A combined corner and edge detector," in *Alvey Vision Conf.*, Vol. 15, p. 50, University of Sheffield Printing Office, Manchester, UK (1988).
7. J. Xiao et al., "Adaptive algorithm for corner detecting based on the degree of sharpness of the contour," *Opt. Eng.* **50**(4), 047008 (2011).
8. J. Lv, G. Deng, and B. Xu, "A new automated image registration method based on corners," in *Multimedia and Signal Processing*, pp. 95–102, Springer, Berlin, Heidelberg (2012).
9. B. Yi et al., "A fast matching algorithm with feature points based on NCC," in *Proc. Int. Academic Workshop on Social Science*, pp. 955–958, Alantis Press, China, Changsha (2013).
10. S. M. Smith and J. M. Brady, "SUSAN—A new approach to low level image processing," *Int. J. Computer Vision* **23**(1), 45–78 (1997).
11. Y. Song and M. Li, "Research on SUSAN based auto-focusing algorithm for optical microscope application," in *Proc. IEEE Int. Conf. Mechatronics and Automation*, pp. 1237–1241, IEEE (2006).
12. K. Voss and H. Suesse, "Affine point pattern matching," *Pattern Recognit.* **2191** 155–162 (2001).
13. H. Chui and A. Rangarajan, "A new point matching algorithm for non-rigid registration," *Comput. Vision Image Underst.* **89**(2), 114–141 (2003).
14. M. Carcassoni and E. Hancock, "Spectral correspondence for point pattern matching," *Pattern Recognit.* **36**(1), 193–204 (2003).
15. T. Caetano et al., "Graphical models and point pattern matching," *IEEE Trans. Pattern Anal. Mach. Intell.* **28**(10), 1646–1663 (2006).
16. H. Zhu et al., "Robust and fast hausdorff distance for image matching," *Opt. Eng.* **51**(1), 017203 (2012).
17. W. Qian et al., "Voting-strategy-based approach to image registration," *OptoElectron. Eng.* **35**(10), 86–91 (2008).
18. G. L. Mohammad Awrangjeb and C. S. Fraser, "Performance comparisons of contour-based detectors," *IEEE Trans. Image Process.* **21**(9), 4167–4179 (2012).
19. M. Awrangjeb and G. Lu, "An improved curvature scale-space corner detector and a robust corner matching approach for transformed image identification," *IEEE Trans. Image Process.* **17**(12), 2425–2441 (2008).
20. M. Awrangjeb, G. Lu, and C. S. Fraser, "A comparative study on contour-based corner detectors," in *Int. Conf. Digital Image Computing: Techniques and Applications*, pp. 92–99, IEEE (2010).
21. M. Awrangjeb and G. Lu, "Techniques for efficient and effective transformed image identification," *J. Visual Commun. Image Represent.* **20**(8), 511–520 (2009).
22. D. Lowe, "Distinctive image features from scale-invariant keypoints," *Int. J. Comput. Vision* **60**(2), 91–110 (2004).
23. Q. Zeng, L. Liu, and J. Li, "Image registration method based on improved Harris corner detector," *Chin. Opt. Lett.* **8**(6), 573–576 (2010).
24. W.-G. Qian and X.-Z. Lin, "Detection algorithm of image corner based on contour sharp degree," *Comput. Eng.* **34**(6), 202–204 (2008).
25. S. Chen, "A corner matching algorithm based on Harris operator," in *Int. Conf. Information Engineering and Computer Science*, pp. 1–2, IEEE (2010).
26. J. Liu et al., "A comparative study of different corner detection methods," in *IEEE Int. Symp. Computational Intelligence in Robotics and Automation*, pp. 509–514 IEEE, Daejeon (2009).
27. M. Wang and X. Deng, "A new right angle corner detection method," in *Int. Conf. Artificial Intelligence and Computational Intelligence*, Vol. 2, pp. 28–30, IEEE, Beijing (2009).

Yue Zhao received her BS degrees in measuring and control technology and instrumentation from Harbin Engineering University in 2009. She is currently working toward a PhD degree at the Department of Automation, Shanghai Jiao Tong University, Shanghai, China. Her research interests include pattern recognition, image processing, face recognition, and sparse representation.

Jianbo Su is a full professor of Shanghai Jiao Tong University. His research interests include robotics, pattern recognition, and human-machine interaction. In these areas, he has published three books, more than 190 technical papers, and is the holder of 15 patents. He has served as an associate editor for *IEEE Transactions on Systems, Man, and Cybernetics*, Part B: Cybernetics, since 2005.

Downloaded From: http://electronicimaging.spiedigitallibrary.org/ on 12/18/2014 Terms of Use: http://spiedl.org/terms